Journal of Superconductivity and Novel Magnetism (2020) 33:625–628
https://doi.org/10.1007/s10948-019-05218-1

ORIGINAL PAPER

Superconductivity in Oxychalcogenide $LaREO_2Bi_3Ag_{0.6}Sn_{0.4}S_6$ (RE = Pr and Nd)

G. C. Kim[1] · M. Cheon[1] · Woojae Choi[2] · D. Ahmad[3] · Yong Seung Kwon[2] · Rockkil Ko[1,4] · Y. C. Kim[1]

Received: 1 July 2019 / Accepted: 11 July 2019 / Published online: 21 August 2019

Abstract

We have investigated the structural, electrical, and magnetic properties of oxychalcogenide $LaREO_2Bi_3Ag_{0.6}Sn_{0.4}S_6$ (RE = Pr and Nd) superconductors. The $LaREO_2Bi_3Ag_{0.6}Sn_{0.4}S_6$ (RE = Pr and Nd) samples are composed of a single $La_2O_2Bi_3AgS_6$ phase without any impurity phase. The superconducting onset temperature of $LaREO_2Bi_3Ag_{0.6}Sn_{0.4}S_6$ (RE = Pr and Nd) is ~ 4.1 K, which is slightly higher than 2.8 K observed for $La_2O_2Bi_3Ag_{0.6}Sn_{0.4}S_6$.

Keywords BiS_2-based superconductor · $La_2O_2Bi_3AgS_6$ · Oxychalcogenide

1 Introduction

Since the discovery of superconductivity (SC) in $Bi_4O_4S_3$ with an onset critical transition temperature of $T_{c,\text{onset}} = 8.60$ K [1], several BiS_2-based layered compounds including $REOBiS_2$ (RE = La, Ce, Pr, Nd, and Yb), $SrFBiS_2$, Bi_2OS_2, and $Bi_3O_2S_3$ have been discovered [2–11]. The crystal structure of the parent compound $REOBiS_2$ is composed of alternate stacks of conducting BiS_2 bilayers and insulating RE_2O_2 blocking layers. Although $REOBiS_2$ is intrinsically an insulator with a band gap, SC was observed by partially substituting O at the RE_2O_2 blocking layers with F, which induces an electron carrier in the BiS_2 layers. From the first-principles band-structure calculation, SC in BiS_2-based compounds is derived from the Bi $6p_x$ and $6p_y$ orbitals [12]. T_c in $REO_{1-x}F_xBiS_2$ is distributed in the range of 2–5 K, depending on RE elements. Among BiS_2-based layered compounds, $LaO_{0.5}F_{0.5}BiS_2$ synthesized under high pressure shows a maximum $T_{c,\text{zero}} \simeq 10.5$ K [13]. In the case of $CeO_{0.5}F_{0.5}BiS_2$ with $T_{c,\text{onset}} \simeq 3.0$ K, the coexistence of SC and ferromagnetism arising from the local moments of Ce at low temperatures was confirmed from the electrical resistivity and magnetization measurements [3, 14].

Recently, Jha et al. [15] reported SC in the layered oxychalcogenide $La_2O_2Bi_3AgS_6$ with $T_c \simeq 0.5$ K. The crystal structure of $La_2O_2Bi_3AgS_6$ is composed of alternate stacks of $LaOBiS_2$-type layers and rock-salt-type (Bi,Ag)S layers. They also observed a broad hump in the temperature dependence of resistivity below $T^* \sim 180$ K, possibly due to the charge density wave (CDW) transition. In $La_2O_2Bi_3Ag_{1-x}Sn_xS_6$, T_c increased and a broad hump in the temperature dependence of resistivity weakened, with increasing Sn content from $x = 0$ to 0.5 [16]. The broad hump in the temperature dependence of resistivity disappeared for $x \geq 0.3$, and the maximum superconducting onset temperature, $T_{c,\text{onset}}$, achieved was 2.8 K at $x = 0.4$.

This paper reports the structural, electrical, and magnetic properties of oxychalcogenide $LaREO_2Bi_3Ag_{0.6}Sn_{0.4}S_6$ (RE = Pr and Nd) superconductors. In $LaREO_2Bi_3Ag_{0.6}Sn_{0.4}S_6$, the lattice parameter c is insensitive with RE = Pr or Nd, but the lattice parameter a decreases monotonically with decreasing ionic radius of RE. The superconducting onset temperature on $LaREO_2Bi_3Ag_{0.6}Sn_{0.4}S_6$ (RE = Pr and Nd), which determined by the electrical resistivity and magnetization measurements, is ~ 4.1 K.

✉ Y. C. Kim
yckim@pusan.ac.kr

[1] Department of Physics, Pusan National University, Busan 46241, South Korea

[2] Department of Emerging Materials Science, DGIST, Daegu, 42988, South Korea

[3] Department of Mathematics and Natural Sciences, North Lake College, Dallas County College District, Irving, TX 75038, USA

[4] Superconductivity Research Center, Korea Electrotechnology Research Institute, Gyeongsangnam-do, South Korea

2 Experimental

Polycrystalline samples of $LaREO_2Bi_3Ag_{0.6}Sn_{0.4}S_6$ (RE = Pr and Nd) were synthesized using a solid state reaction method. Powders of La_2O_3 (99.99 %), Pr_2O_3 (99.9 %), Nd_2O_3 (99.9 %), La_2S_3 (99.9 %), Ag_2O (99.9 %), Bi (99.999 %), Sn (99.8 %), and S (99.5 %) with a nominal composition of $LaREO_2Bi_3Ag_{0.6}Sn_{0.4}S_6$ were mixed, pressed into pellets, and sealed in an evacuated quartz tube. As mentioned in Refs. [15] and [16], the sintering temperature was 725 °C with a sintering period of 15 h. The sintering procedure was repeated for one more time to achieve a homogeneous combination reaction with an intermediate grinding with the same sintering temperature and period. On the other hand, the properties of the samples, obtained using two sintering steps at 725 °C, were not acceptable, which may be caused by the two sintering steps at high temperature. The optimal sintering temperatures for each sample were determined by examining the XRD results and magnitude of zero field-cooled magnetization at 2 K. As a result, after first sintering at 720 °C for 15 h, the samples were sintered at 670 °C in the second step for 15 h to minimize the loss of metallic elements such as Bi, Ag, and Sn. Attempts were also made to synthesize $RE_2O_2Bi_3Ag_{0.6}Sn_{0.4}S_6$ (RE = Ce and Nd) and $LaREO_2Bi_3Ag_{0.6}Sn_{0.4}S_6$ (RE = Y, Ce, and Sm) samples using the our method and the procedure suggested in Refs. [15] and [16]. Unfortunately, these samples contained excessive impurities induced by the loss of metallic elements.

The phase purity of the prepared samples was examined by X-ray diffraction (XRD) using a Cu Kα radiation at room temperature. The electrical resistivity down to 2 K was measured by a standard four-probe method in a commercial Quantum Design PPMS-14 system. The magnetic properties were measured over the temperature range, 2 K to 8 K, using the Physical Property Measurement System (PPMS, Quantum Design).

3 Results and Discussion

Figure 1a presents the room temperature XRD pattern of polycrystalline $LaREO_2Bi_3Ag_{0.6}Sn_{0.4}S_6$ (RE = Pr and Nd) samples. The structure of $La_2O_2Bi_3AgS_6$ is tetragonal with the space group $P4/nmm$ [17]. As shown in Fig. 1a, the XRD peaks for the $LaREO_2Bi_3Ag_{0.6}Sn_{0.4}S_6$ (RE = Pr and Nd) samples are indexed to the $La_2O_2Bi_3AgS_6$ phase, indicating that the samples are composed of a single phase without an impurity phase. Figure 1 b shows the (006) peaks on $LaREO_2Bi_3Ag_{0.6}Sn_{0.4}S_6$ (RE = Pr and Nd). The shift in the (006) peak was not noticeable,

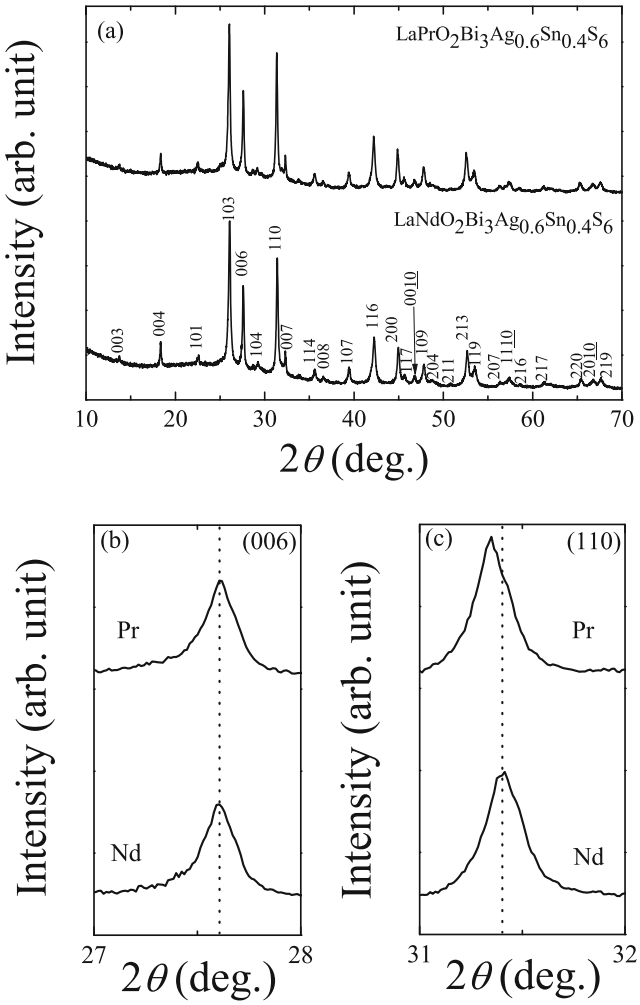

Fig. 1 **a** The room temperature XRD patterns of polycrystalline $LaREO_2Bi_3Ag_{0.6}Sn_{0.4}S_6$ (RE = Pr and Nd). The XRD patterns near to **b** (006) and **c** (110) peaks of $LaREO_2Bi_3Ag_{0.6}Sn_{0.4}S_6$ (RE = Pr and Nd)

suggesting that the lattice parameter c is not sensitive to RE = Pr or Nd. On the other hand, the (110) peak shifts toward a higher angle side as the RE is changed from Pr to Nd (see, Fig. 1c), i.e., the lattice parameter a decreases with decreasing ionic radius of RE from 1.179 Å (Pr^{3+}) to 1.163Å (Nd^{3+}) [18].

The estimated lattice parameters based on the XRD peaks are $a = 4.0320$ Å and $c = 19.37$ Å for $LaPrO_2Bi_3Ag_{0.6}Sn_{0.4}S_6$ and $a = 4.024$ Å and $c = 19.37$ Å for $LaNdO_2Bi_3Ag_{0.6}Sn_{0.4}S_6$. The $c = 19.37$ Å for $LaREO_2Bi_3Ag_{0.6}Sn_{0.4}S_6$ (RE = Pr and Nd) is shorter than $c = 19.45$ Å on $La_2O_2Bi_3Ag_{0.6}Sn_{0.4}S_6$ [16]. The a decreases monotonically from 4.065 Å [16], to 4.0320 Å to 4.024 Å as RE goes from La to Pr to Nd, as mentioned above.

Figure 2 shows the temperature dependence of the electrical resistivity, $\rho(T)$, of polycrystalline $LaREO_2Bi_3$

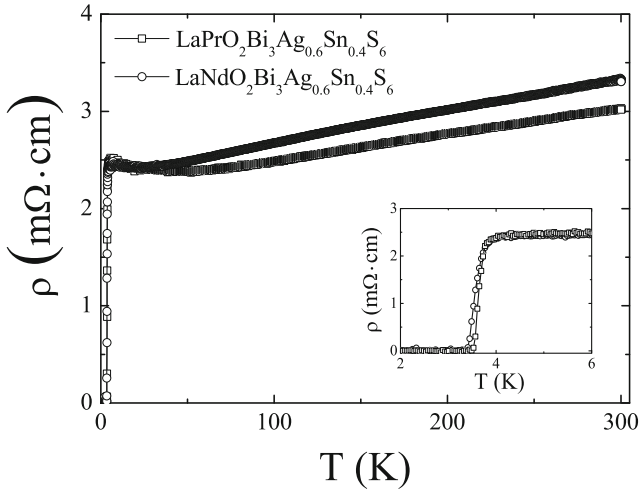

Fig. 2 Temperature dependence of the electrical resistivity $\rho(T)$ of polycrystalline $LaREO_2Bi_3Ag_{0.6}Sn_{0.4}S_6$ (RE = Pr and Nd) samples. The inset shows an enlargement of the region close to T_c

$Ag_{0.6}Sn_{0.4}S_6$ (RE = Pr and Nd). As shown in Fig. 2, ρ(300 K) for the $LaPrO_2Bi_3Ag_{0.6}Sn_{0.4}S_6$ ($\sim$ 3.0 mΩ·cm) and $LaNdO_2Bi_3Ag_{0.6}Sn_{0.4}S_6$ ($\sim$ 3.3 mΩ·cm) is slightly smaller than that ($\sim$ 3.5 mΩ·cm) of $La_2O_2Bi_3Ag_{0.6}Sn_{0.4}S_6$ [16]. The $\rho(T)$ of $La_2O_2Bi_3Ag_{0.6}Sn_{0.4}S_6$ was reported to show simple metallic behavior at the normal state below 300 K, which was then followed by an upturn at $\sim$ 100 K upon lowering temperature [16]. The $LaREO_2Bi_3Ag_{0.6}Sn_{0.4}S_6$ (RE = Pr and Nd) exhibits the upturn behavior after a simple metallic behavior upon lowering temperature. On the other hand, the upturn trend in $\rho(T)$ weakens progressively and the upturn temperature decreases from $\sim$ 100 K (La) to $\sim$ 50 K (Pr), and finally to $\sim$ 25 K (Nd), accompanied by an increase in $d\rho/dT$ before the upturn in $\rho(T)$ at the normal state, as RE goes from La to Nd.

The inset in Fig. 2 shows a plot of $\rho(T)$ over the region close to T_c on polycrystalline $LaREO_2Bi_3Ag_{0.6}Sn_{0.4}S_6$ (RE = Pr and Nd). Both the $LaPrO_2Bi_3Ag_{0.6}Sn_{0.4}S_6$ and $LaNdO_2Bi_3Ag_{0.6}Sn_{0.4}S_6$ samples exhibit the superconducting onset temperature of $T_{c,\mathrm{onset}} \simeq 4.1$ K, which is higher than that ($\simeq$ 2.8 K) of $La_2O_2Bi_3Ag_{0.6}Sn_{0.4}S_6$ [16]. However, $T_{c,\mathrm{zero}}$ ($\simeq$ 3.5 K) of $LaPrO_2Bi_3Ag_{0.6}Sn_{0.4}S_6$ is slightly higher than that ($\simeq$ 3.4 K) of $LaNdO_2Bi_3Ag_{0.6}Sn_{0.4}S_6$ and that ($\simeq$ 2.4 K) of $La_2O_2Bi_3Ag_{0.6}Sn_{0.4}S_6$ as shown in the inset of Fig. 2 [16].

Figure 3a and b shows the temperature dependence of zero field-cooled (ZFC) and field-cooled (FC) magnetizations, M_{ZFC} and M_{FC}, of the polycrystalline $LaREO_2Bi_3Ag_{0.6}Sn_{0.4}S_6$ (RE = Pr and Nd) samples, which is measured under an applied magnetic field of $H = 10$ Oe down to 2 K.

The magnitude of M_{ZFC} at 2 K ($\simeq -0.09$ emu/g) of $LaPrO_2Bi_3Ag_{0.6}Sn_{0.4}S_6$, given in Fig. 3a, is almost 1.5× larger than that ($\simeq -0.06$ emu/g) of $PrO_{0.5}F_{0.5}BiS_2$ measured at $H = 5$ Oe. The M_{FC}, which is measured under a low field of $H = 10$ Oe, features a paramagnetic signal at low temperatures with a transition at $\sim$ 4.2 K, as shown in the upper inset of Fig. 3b. Moreover, M_{ZFC} around T_c is also paramagnetic, displaying a positive peak over a narrow temperature range below T_c, which is followed by a diamagnetic response at lower temperatures. The positive peak in M_{ZFC} below T_c has also been

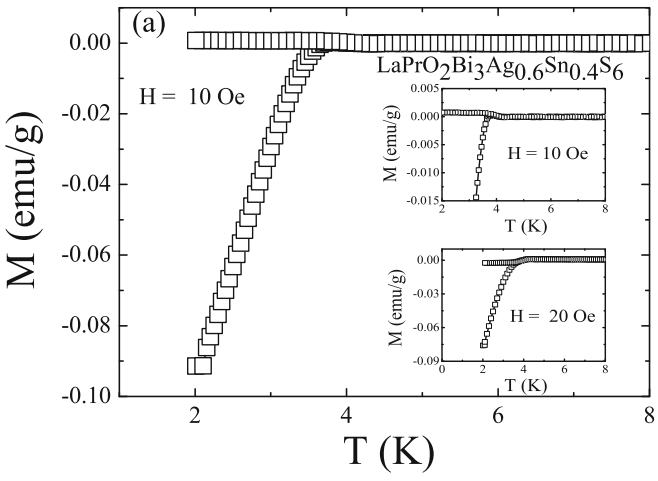

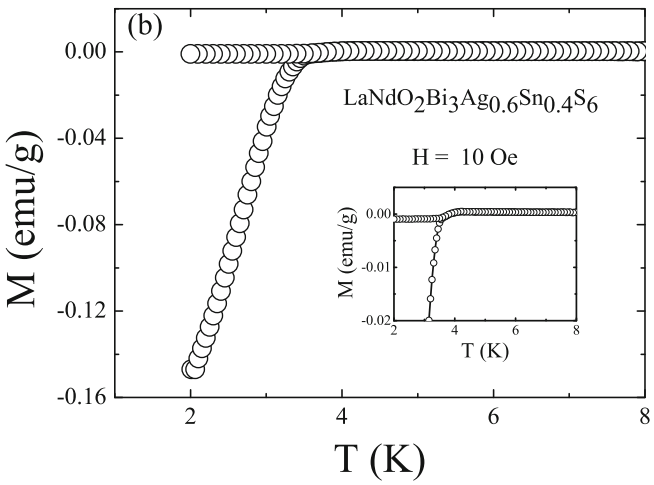

Fig. 3 **a** Temperature dependence of M_{ZFC} and M_{FC} on polycrystalline $LaPrO_2Bi_3Ag_{0.6}Sn_{0.4}S_6$ sample under $H = 10$ Oe. The upper and lower insets show an enlargement of the region close to T_c and temperature dependence of M_{ZFC} and M_{FC} under $H = 10$ Oe, respectively. **b** Temperature dependence of M_{ZFC} and M_{FC} on polycrystalline $LaNdO_2Bi_3Ag_{0.6}Sn_{0.4}S_6$ sample under $H = 10$ Oe. The inset show an enlargement of the region close to T_c

observed in polycrystalline $Bi_2Sr_2CaCu_2O_8$ (Bi-2212), Nb disks, MgB_2, and Pb [19–24]. Such M_{ZFC} and M_{FC} features in superconductors are generally referred to as the paramagnetic Meissner effect (PME). Fang et al. [25] observed the putative PME in samples with $x = 0.1$ and 0.5 of $La_{1-x}Sm_xO_{0.5}F_{0.5}BiS_2$. The putative PME in the present $LaPrO_2Bi_3Ag_{0.6}Sn_{0.4}S_6$ sample disappears as the magnetization is measured under $H = 20$ Oe (see the lower inset in Fig. 3a). The disappearance of PME by the increase in magnetic field is common to other superconductors, such as Bi-2212 showing PME. From the lower inset in Fig. 3a without the putative PME, the superconducting transition temperature is $T_c \simeq 4.2$ K, which is similar to $T_{c,\mathrm{onset}}$ in $\rho(T)$. This is consistent with the paramagnetic transition temperature of M_{FC} measured under $H = 10$ Oe in $LaPrO_2Bi_3Ag_{0.6}Sn_{0.4}S_6$, and higher than $T_c \simeq 3.7$ K of $PrO_{0.5}F_{0.5}BiS_2$ [6].

$LaNdO_2Bi_3Ag_{0.6}Sn_{0.4}S_6$ (Fig. 3b) exhibits the general superconducting transition without the putative PME observed in $LaPrO_2Bi_3Ag_{0.6}Sn_{0.4}S_6$. From the temperature dependence of M_{ZFC} shown in Fig. 3b, it is expected that the values of M_{ZFC} appear to be saturated at $T < 2$ K, which means that the bulk SC can be achieved. The shielding volume fraction of $LaPrO_2Bi_3Ag_{0.6}Sn_{0.4}S_6$ ($LaNdO_2Bi_3Ag_{0.6}Sn_{0.4}S_6$) estimated from $4\pi\chi$(ZFC) at 2 K is nearly 35% (98%). From the inset in Fig. 3b, T_c of $LaNdO_2Bi_3Ag_{0.6}Sn_{0.4}S_6$ is 4.1 K, which is lower than $T_c \simeq 5.0$ K of $NdO_{0.5}F_{0.5}BiS_2$ showing the highest T_c among the BiS_2-based compounds synthesized at ambient pressure [4]. The absence of PME for $LaNdO_2Bi_3Ag_{0.6}Sn_{0.4}S_6$ (Fig. 3b) at 10 Oe indicates clearly that the positive FC for $LaPrO_2Bi_3Ag_{0.6}Sn_{0.4}S_6$ is PME.

4 Summary

In summary, this study examined the structural, electrical, and magnetic properties of oxychalcogenide $LaREO_2Bi_3Ag_{0.6}Sn_{0.4}S_6$ (RE = Pr and Nd) superconductors. The lattice parameter c (a) of $LaREO_2Bi_3Ag_{0.6}Sn_{0.4}S_6$ (RE = Pr and Nd) samples with a single phase of $La_2O_2Bi_3AgS_6$ is insensitive on RE = Pr or Nd (decreases monotonically with decreasing ionic radius of RE). The superconducting onset temperature of $LaREO_2Bi_3Ag_{0.6}Sn_{0.4}S_6$ (RE = Pr and Nd) is ~ 4.1 K, which is slightly higher than 2.8 K of $La_2O_2Bi_3Ag_{0.6}Sn_{0.4}S_6$.

Funding Information This work was supported by a 2-Year Research Grant of Pusan National University.

References

1. Mizuguchi, Y., Fujihisa, H., Gotoh, Y., Suzuki, K., Usui, H., Kuroki, K., Demura, S., Takano, Y., Izawa, H., Miura, O.: Phys. Rev. B **86**, 220510 (2012)
2. Lee, J., Stone, M.B., Huq, A., Yildirim, T., Ehlers, G., Mizuguchi, Y., Miura, O., Takano, Y., Deguchi, K., Demura, S., Lee, S.-H.: Phys. Rev. B **87**, 205134 (2013)
3. Xing, J., Li, S., Ding, X., Yang, H., Wen, H.-H.: Phys. Rev. B **86**, 214518 (2012)
4. Demura, S., Mizuguchi, Y., Deguchi, K., Okazaki, H., Hara, H., Watanabe, T., Denholme, S.J., Fujioka, M., Ozaki, T., Fujihisa, H., Gotoh, Y., Miura, O., Yamaguchi, T., Takeya, H., Takano, Y.: J. Phys. Soc. Jpn. **82**, 033708 (2013)
5. Kajitani, J., Deguchi, K., Hiroi, T., Omachi, A., Demura, S., Takano, Y., Miura, O., Mizuguchi, Y.: J. Phys. Soc. Jpn. **83**, 065002 (2014)
6. Jha, R., Tiwari, B., Awana, V.P.S.: J. Phys. Soc. Jpn. **83**, 063707 (2014)
7. Yazici, D., Huang, K., White, B.D., Chang, A.H., Friedman, A.J., Maple, M.B.: Philos. Mag. **93**, 673 (2013)
8. Shao, J., Yao, X., Liu, Z., Pi, L., Tan, S., Zhang, C., Zhang, Y.: Supercond. Sci. Technol. **28**, 015008 (2015)
9. Phelan, W.A., Wallace, D.C., Arpino, K.E., Neilson, J.R., Livi, K.J., Seabourne, C.R., Scott, A.J., McQueen, T.M.: J. Am. Chem. Soc. **135**, 5372 (2013)
10. Shao, J., Liu, Z., Yao, X., Pi, L., Tan, S., Zhang, C., Zhang, Y.: Phys. Status Solidi RRL **8**, 845 (2014)
11. Li, L., Parker, D., Babkevich, P., Yang, L., Ronnow, H.M., Sefat, A.S.: Phys. Rev. B **91**, 104511 (2015)
12. Morice, C., Artacho, E., Dutton, S.E., Molnar, D., Kim, H.-J., Saxena, S.S.: J. Phys.: Condens. Matter **27**, 135501 (2015)
13. Mizuguchi, Y., Hiroi, T., Kajitani, J., Takatsu, H., Kadowaki, H., Miura, O.: J. Phys. Soc. Jpn. **83**, 053704 (2014)
14. Lee, J., Demura, S., Stone, M.B., Iida, K., Ehlers, G., dela Cruz, C.R., Matsuda, M., Deguchi, K., Takano, Y., Mizuguchi, Y., Miura, O., Louca, D., Lee, S.-H.: Phys. Rev. B **90**, 224410 (2014)
15. Jha, R., Goto, Y., Higashinaka, R., Matsuda, T.D., Aoki, Y., Mizuguchi, Y.: J. Phys. Soc. Jpn. **87**, 083704 (2018)
16. Jha, R., Goto, Y., Matsuda, T.D., Aoki, Y., Nagao, M., Tanaka, I., Mizuguchi, Y.: arXiv:1810.08404
17. Hijikata, Y., Abe, T., Moriyoshi, C., Kuroiwa, Y., Goto, Y., Miura, A., Tadanaga, K., Wang, Y., Miura, O., Mizuguchi, Y.: J. Phys. Soc. Jpn. **86**, 124802 (2017)
18. Shannone, R.D.: Acta Cryst. **A32**, 751 (1976)
19. Chaban, I.A.: J. Supercond. **13**, 1011 (2000)
20. Thompson, D.J., Minhaj, M.S.M., Wenger, L.E., Chen, J.T.: Phys. Rev. Lett. **75**, 529 (1995)
21. Braunisch, W., Knauf, N., Kataev, V., Neuhausen, S., Grutz, A., Kock, A., Roden, B., Khomskii, D., Wohlleben, D.: Phys. Rev. Lett. **68**, 1908 (1992)
22. Sozeri, H., Dorosinskii, L., Topal, U., Ercan, I.: Phys. C **408–410**, 109 (2004)
23. Yuan, S., Ren, L., Li, F.: Phys. Rev. B **69**, 092509 (2004)
24. Papadopoulou, E.L., Nordblad, P., Svedlindh, P., Schoneberger, R., Gross, R.: Phys. Rev. Lett. **82**, 173 (1999)
25. Fang, Y., Yazici, D., White, B.D., Maple, M.B.: Phys. Rev. B **91**, 064510 (2015)